

Fluoride-free synthesis of high-silica RHO zeolite for the highly selective synthesis of methylamine

Yufei Wang,^{a#} Jinfeng Han,^{a#} Keyan Jin,^a Shuang Liu,^a Qiang Li,^a Pan Hou,^a Shiping Liu,^b Qi Song,^c Zhendong Wang,^c Peng Tian,^{b*} and Wenfu Yan^{a*}

^aState Key Laboratory of Inorganic Synthesis and Preparative Chemistry, College of Chemistry, Jilin University, 2699 Qianjin Street, Changchun 130012, China.

^bNational Engineering Research Center of Lower-Carbon Catalysis, Dalian National Laboratory for Clean Energy, Dalian Institute of Chemical Physics, Chinese Academy of Sciences, Dalian 116023, China

^cState Key Laboratory of Green Chemical Engineering and Industrial Catalysis, Sinopec Shanghai Research Institute of Petrochemical Technology Co., Ltd., Shanghai 201208, China

#These authors contributed equally to this work.

***Corresponding Author:**

E-mail: tianpeng@dicp.ac.cn (Peng Tian), yanw@jlu.edu.cn (Wenfu Yan).

Table of contents in Supporting Information

1. Experimental Section	3
1.1 Chemical and Materials	3
1.2 Synthesis of RHO Seeds.....	3
1.3 Preparation of the OSDA	3
1.4 Synthesis of RHO-8.7.....	3
1.5 Synthesis of RHO-7.3.....	4
1.6 Synthesis of RHO-7.9C	4
1.7 Synthesis of RHO-6.7C	4
1.8 Ion Exchange	4
2. Characterizations	5
3. Catalysis	6
Fig. S1. TG curves of the as-synthesized zeolites of RHO-8.7, RHO-7.3, RHO-7.9C, RHO-6.7C, and RHO seeds.	7
Fig. S2. Simulated and experimental XRD pattern of the isolated solid sample upon 2 d heating in the crystallization of RHO-8.7 and RHO-7.3	7
Fig. S3. Simulated XRD patterns and experimental XRD patterns of parent UZM-12 and the product of the interzeolite conversion of UZM-12; parent SSZ-39 and the products of the interzeolite conversion of SSZ-39.	8
Fig. S4. Simulated XRD patterns and experimental XRD patterns of parent SSZ-13 (Si/Al = 35) and the product RHO zeolite; parent SSZ-13 (Si/Al = 10) and the product in the synthesis of RHO-8.7 (RHO-8.7-no seed: the product of Run 3, RHO-8.7-eq: the product of Run 4); parent SSZ-13 (Si/Al = 8) and the product in the synthesis of RHO-7.3 (RHO-7.3-no seed: the product of Run 6, RHO-7.3-eq: the product of Run 7)..	8
Fig. S5. Phase diagrams of RHO-8.7 and RHO-7.3 synthesized from different gel compositions at 150 °C 4 d.....	8
Fig. S6. NH ₃ -TPD profiles of H-RHO-8.7, H-RHO-7.9C, H-RHO-7.3 and H-RHO-6.7C	9
Table S1. Textural properties of high-silica H-RHO samples	10
Table S2. The acidic properties of H-RHO-8.7, H-RHO-7.9C, H-RHO-7.3 and H-RHO-6.7C	10
References	11

1. Experimental Section

1.1 Chemical and Materials

18-crown-6 (Energy Chemical; 99 wt%), NaAlO₂ (Sinopharm Chemical Reagent Co., Ltd; Al₂O₃ ≥ 41.0%), NaOH (Tianjin Fuchen; NaOH ≥ 96.0%), CsOH (3A; 50 wt% solution in water), Ludox AS-40 (Aldrich; 40 wt%, suspension in water), Pseudo-boehmite (Sasol; 72.7 wt%), NaF (Xilong Scientific; ≥ 98 wt%), SSZ-13 (Luoyang JALON Micro-nano New Materials Co., Ltd; Si/Al = 10), SSZ-13 (Luoyang JALON Micro-nano New Materials Co., Ltd; Si/Al = 8), NH₄Cl (Tianjin Fuchen), Deionized water.

1.2 Synthesis of RHO Seeds

RHO seeds were synthesized using a gel composition consisting of 1.8 Na₂O: 0.3 Cs₂O: 1.0 Al₂O₃: 10 SiO₂: 0.5 (18-crown-6): 100 H₂O.¹ To prepare this, 16.22 g of deionized water, 0.64 g of NaOH, 3.60 g of CsOH, 2.64 g of 18-crown-6, 4.25 g of NaAlO₂, and 30.04 g of AS-40 were sequentially added and stirred for 24 h at ambient temperature. The crystallization process was then conducted at 110 °C for 4 d in a 100 mL stainless steel autoclave in static conditions.

Afterwards, the mixture was separated, washed twice with deionized water, and dried overnight at 80 °C. The resulting sample was calcined at 550 °C under air atmosphere for 6 h to eliminate organic species, yielding a white powder, which was collected and utilized as **RHO** seeds in subsequent procedures.

1.3 Preparation of OSDA

The synthetic procedure was based on the published findings of Ke et al.² In a 50 mL glass bottle, 21.2 g of 18-crown-6, 2.8 g of NaOH, 14.0 g of deionized water, and 8.0 g of CsOH were sequentially added, resulting in a molar composition of the mixture of 0.081 (18-crown-6): 0.070 NaOH: 1.00 H₂O: 0.027 CsOH. The mixture was stirred in a water bath at 80 °C for 3 h. After cooling to ambient temperature under static conditions, the clear phase, exhibiting a yellow coloration on the upper surface, was separated and utilized as the organic directing-directing agent (OSDA) in subsequent synthetic processes. According to the literature,² the formula of the OSDA is (NaOH)_{1.4}·(CsOH)·(18-crown-6)_{2.2}·(H₂O)_{10.2}.

1.4 Synthesis of RHO-8.7

RHO-8.7 was synthesized using a gel composition comprising 1.0 Al₂O₃: 20 SiO₂: 2.8 OSDA: 100 H₂O: 12% seeds (12 wt% of SiO₂). To prepare, 7.5 g of SSZ-13 (Si/Al = 10, calcined at 600 °C for 6 h to remove organic species) and 0.8 g of **RHO** seeds were added to 10 g of deionized water. Subsequently, 15.5 g of OSDA was introduced into the mixture, which was then stirred for 24 h at ambient temperature.

The crystallization process was conducted at 150 °C for 4 d in a 50 mL stainless steel autoclave in static conditions. Following separation, the resulting product was washed twice with deionized water and dried overnight at 80 °C, yielding a white powder sample denoted as **RHO-8.7**. This sample was then calcined at 600 °C for 6 h to eliminate organic species.

1.5 Synthesis of RHO-7.3

RHO-7.3 was synthesized using a gel composition consisting of 1.0 Al₂O₃: 16 SiO₂: 2.2 OSDA: 85 H₂O: 10% seeds (10 wt% of SiO₂). To begin the synthesis, 5.2 g of SSZ-13 (Si/Al = 8, calcined at 600 °C for 6 h to remove organic species) and 0.5 g of **RHO** seeds were combined with 7 g of deionized water. Subsequently, 10 g of OSDA was added to the mixture, which was then stirred for 24 h at ambient temperature.

The crystallization process took place at 150 °C for 4 d in a 50 mL stainless steel autoclave in static conditions. Upon completion, the mixture was separated, and the resulting product was washed twice with deionized water before being dried overnight at 80 °C. The resulting white powder sample was designated as **RHO-7.3**, and it was subjected to further treatment by calcination at 600 °C under air atmosphere for 6 h to remove organic species.

1.6 Synthesis of **RHO-7.9C**

As per the method outlined by Ke et al.,³ high-silica **RHO** zeolites with a Si/Al ratio of 7.9 were synthesized using a gel composition comprising 1.0 Na₂O: 1.0 Al₂O₃: 25 SiO₂: 0.5 NaF: 4.0 OSDA: 160 H₂O: 3% seeds (3 wt% of SiO₂). The synthesis process involved adding 0.56 g of NaAlO₂, 0.05 g of NaF, and 0.1 g of **RHO** seeds to 6.6 g of deionized water. Subsequently, 9.0 g of OSDA and 8.45 g of Ludox AS-40 were introduced into the mixture sequentially, followed by stirring for 24 h at ambient temperature.

Crystallization was performed at 140 °C for 6 d in a 100 mL stainless-steel autoclave under static conditions. After separation, the resulting product underwent two washes with deionized water and was then dried overnight at 80 °C. The resulting white powder sample was identified as **RHO-7.9C** and underwent further treatment through calcination at 600 °C under air atmosphere for 6 h to remove organic species.

1.7 Synthesis of **RHO-6.7C**

As per the methodology outlined by Ke et al.,³ high-silica **RHO** zeolites with a Si/Al ratio of 7.9 were synthesized using a gel composition consisting of 1.0 Na₂O: 1.0 Al₂O₃: 20 SiO₂: 3.3 OSDA: 130 H₂O: 3% seeds (3 wt% of SiO₂). The synthesis procedure involved adding 0.7 g of NaAlO₂ and 0.1 g of **RHO** seeds to 6.6 g of deionized water. Subsequently, 9.0 g of OSDA and 8.45 g of Ludox AS-40 were sequentially introduced into the mixture, followed by stirring for 24 h at room temperature.

Crystallization was conducted at 140 °C for 6 d in a 100 mL stainless-steel autoclave under static conditions. Upon separation, the resulting product underwent two washes with deionized water before being dried at 80 °C overnight. The resulting white powder sample was labeled as **RHO-6.7C** and underwent further processing through calcination at 600 °C under air atmosphere for 6 h to eliminate organic species.

1.8 Ion Exchange

The calcined **RHO** zeolite was added to a 3 mol/L NH₄Cl solution at a ratio of solid (g) to liquid (mL) = 1:30. The mixture was stirred in a water bath at 80 °C for 5 h, repeated four times. After each cycle, the solid was separated, washed, and dried at 80 °C. Subsequently, it was calcined at 550 °C under air atmosphere for 4 h.

2. Characterizations

Powder X-ray diffraction (PXRD) analyses were performed by Rigaku D/Max 2550 X-ray diffractometer in the scanning range of 2θ between 4° and 40° with $12^\circ/\text{min}$ using copper $K\alpha$ as the source of radiation ($\lambda=1.5418 \text{ \AA}$). PXRD data used for Rietveld refinement was collected on the STOE STADI PESSENTIAL X-ray diffractometer equipped with a Mythen II detector in the Debye-Scherrer mode with Cu $K\alpha 1$ radiation ($\lambda=1.5406 \text{ \AA}$) in the Debye-Scherrer mode. The relative crystallinity corresponds to:¹

$$\text{Relative Crystallinity} = \frac{\sum A(\text{characteristic peaks})}{\sum A(\text{characteristic peaks of reference sample})} \times 100\%$$

where A is the peak area of a characteristic peak.

Characteristic peaks of **RHO** zeolite at $2\theta = 8.4^\circ, 11.9^\circ, 14.6^\circ, 18.8^\circ, 22.3^\circ, 23.9^\circ, 26.7^\circ, 29.2^\circ, 32.9^\circ,$ and 37.2° were taken into account for the calculation of relative crystallinity of **RHO** zeolite. Characteristic peaks of SSZ-13 at $9.7^\circ, 13.1^\circ, 14.2^\circ, 18.0^\circ, 23.4^\circ, 26.3^\circ, 28.5^\circ,$ and 31.1° were used for the calculation of relative crystallinity of SSZ-13. Fourier transform infrared (FT-IR) spectra were recorded between 400 to 4000 cm^{-1} by using Bruker VERTEXV 80 V spectrometer. The morphology and microstructure were obtained with field emission scanning electron microscopy (SEM, JSM-7800F). Thermogravimetric (TG) analysis was carried out on a TA TGA Q500 unit with a heating rate of $10 \text{ }^\circ\text{C min}^{-1}$ in air. The chemical compositions were determined by a Thermo Scientific iCAP 7600 DUO ICP-OES. The local environments of atoms were analyzed by ^{27}Al and ^{29}Si solid-state magic angle spinning nuclear magnetic resonance (MAS NMR) measurements on a Bruker Avance NEO system with 14.09 T magnetic field intensity. The calculation of Si/Al ratio from NMR refers to the formula as follows:⁴

$$(Si/Al)_{NMR} = \frac{A_{Si(4Al)} + A_{Si(3Al)} + A_{Si(2Al)} + A_{Si(1Al)} + A_{Si(0Al)}}{A_{Si(4Al)} + 0.75A_{Si(3Al)} + 0.5A_{Si(2Al)} + 0.25A_{Si(1Al)}}$$

where $A_{Si(nAl)}$ is the peak area of Si(n Al) signal.

N_2 adsorption/desorption measurements were carried out on BSD-660M A6MB6M at 77 K . The textural properties including total surface area, external surface area, and micropore volume were measured using Brunauer-Emmett-Teller (BET) equation and t-plot method, respectively. The total pore volume was obtained from the capacity of N_2 adsorbed at $P/P_0 = 0.99$. The temperature-programmed desorption of ammonia (NH_3 -TPD) measurements were carried out on a Micromeritics AutoChem II 2920. The elemental analysis was carried on Elementar vario MACRO cube CHNS elemental analyzer.

3. Catalysis

Selective synthesis of methylamine was conducted under atmospheric pressure in a fixed-bed quartz tubular reactor. The zeolites were pelletized, crushed, and sieved into 40-60 mesh size, then activated at 380 °C for 1 h under a nitrogen flow of 50 mL/min. Following pre-treatment, the catalysts were exposed to a feed gas mixture composed of ammonia and methanol (introduced into the reactor by nitrogen). The reaction temperature ranged from 250 to 400 °C, and the weight hourly space velocity (WHSV) of methanol varied from 0.813 to 4.3 h⁻¹.

Product analysis was performed using an Agilent 7890A gas chromatograph equipped with a flame ionization detector and a CP-Volamine capillary column, enabling online monitoring of the products. The initial data collection commenced immediately after the introduction of the feed gas into the reactor and continued for 0.5 h.

For the severer conditions, catalytic experiments were conducted in the reactor under a pressure of 2.0 MPa. A 1.0 g portion of the calcined sample (20-60 mesh) was loaded into the reactor along with glass beads to a total volume of 2 mL. Subsequently, a liquid mixture of ammonia and methanol, with a weight ratio of 1/1 (molar ratio of 1.9/1), was introduced into the reactor at a flow rate of 23.4 mL/h. The reaction temperature was maintained at 350 °C, and the liquid hourly space velocity (LHSV) of the mixed liquid was 11.7 h⁻¹ (equal to the gas hourly space velocity (GHSV) of the mixed gas at 7488 h⁻¹). Data collection began after the introduction of the mixed liquid into the reactor for 2.0 h. Methanol conversion and the selectivity of methylamine were calculated according to the following method:⁵

$$\text{MeOH conversion} = \frac{\text{moles of MeOH (in)} - \text{moles of MeOH (out)}}{\text{moles of MeOH (in)}} \times 100\%$$

$$\text{selectivity of MMA} = \frac{\text{moles of MMA}}{\text{moles of products detected}} \times 100\%$$

$$\text{selectivity of DMA} = \frac{\text{moles of DMA}}{\text{moles of products detected}} \times 100\%$$

$$\text{selectivity of TMA} = \frac{\text{moles of TMA}}{\text{moles of products detected}} \times 100\%$$

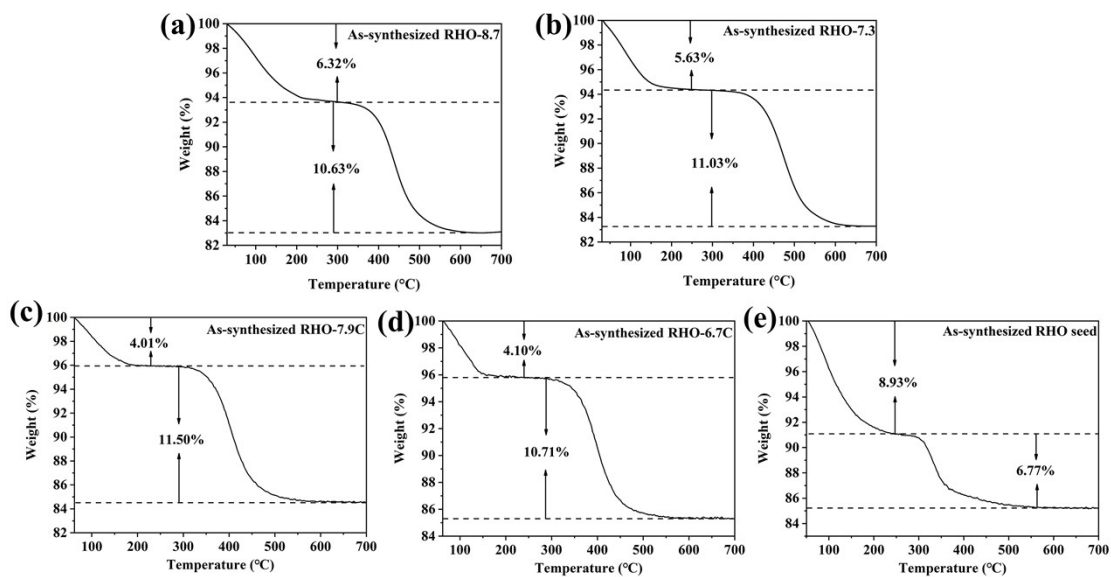


Fig. S1. TG curves of the as-synthesized zeolites of (a) **RHO-8.7**, (b) **RHO-7.3**, (c) **RHO-7.9C**, (d) **RHO-6.7C**, and (e) **RHO seed**.

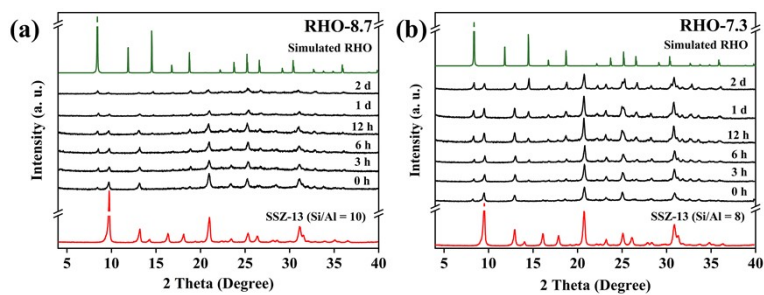


Fig. S2. Simulated and experimental XRD pattern of the isolated solid sample upon 2 d heating in the crystallization of (a) **RHO-8.7** and (b) **RHO-7.3**.

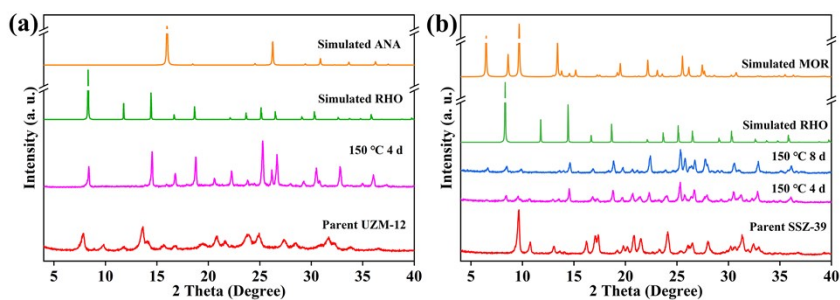


Fig. S3. Simulated XRD patterns and experimental XRD patterns of (a) parent UZM-12⁶ and the product of the interzeolite conversion of UZM-12; (b) parent SSZ-39⁷ and the products of the interzeolite conversion of SSZ-39.

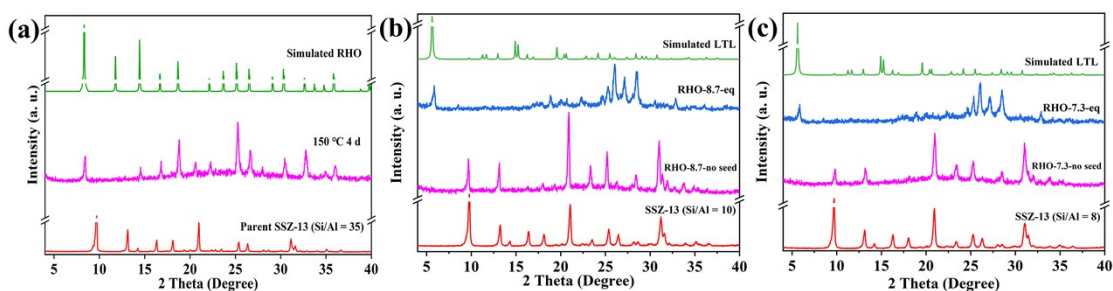


Fig. S4. (a) Simulated XRD patterns and experimental XRD patterns of (a) parent SSZ-13 (Si/Al = 35)⁸ and the product **RHO** zeolite; (b) parent SSZ-13 (Si/Al = 10) and the product in the synthesis of **RHO-8.7** (**RHO-8.7-no seed**: the product of Run 3, **RHO-8.7-eq**: the product of Run 4); (c) parent SSZ-13 (Si/Al = 8) and the product in the synthesis of **RHO-7.3** (**RHO-7.3-no seed**: the product of Run 6, **RHO-7.3-eq**: the product of Run 7).

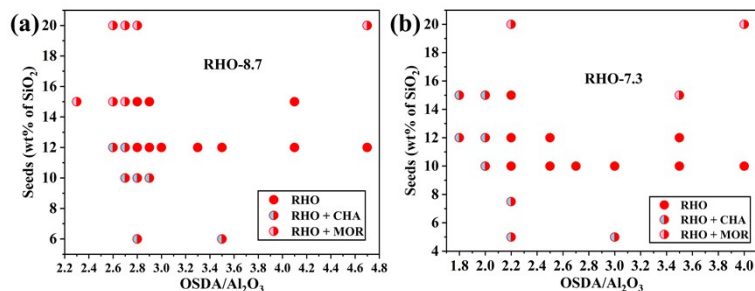


Fig. S5. Phase diagrams of (a) **RHO-8.7** and (b) **RHO-7.3** synthesized from various gel compositions at 150 °C 4 d.

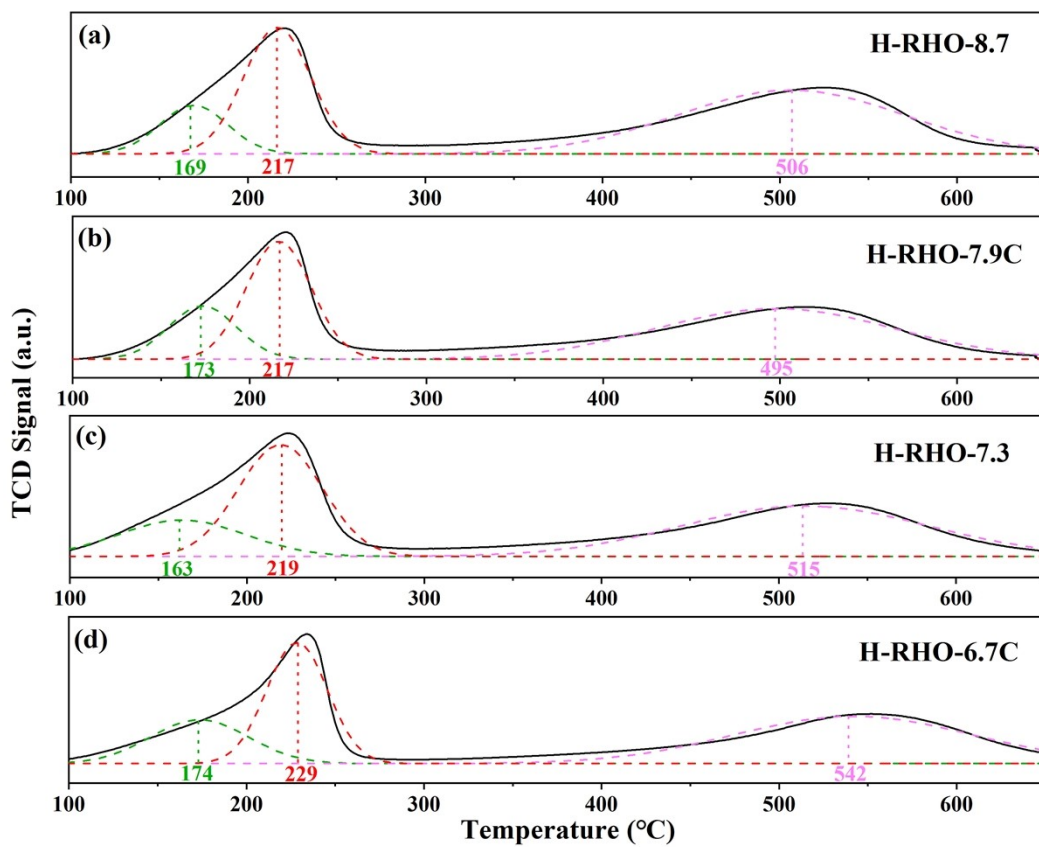


Fig. S6. NH_3 -TPD profiles of (a) H-RHO-8.7, (b) H-RHO-7.9C, (c) H-RHO-7.3, and (d) H-RHO-6.7C.

Table S1. Textural properties of high-silica H-RHO samples

Sample	S _{BET} (m ² /g)	S _{micro} (m ² /g)	V _{total} (cm ³ /g)	V _{micro} (cm ³ /g)
H-RHO-8.7	833	812	0.363	0.313
H-RHO-7.9C	870	850	0.361	0.323
H-RHO-7.3	911	893	0.367	0.338
H-RHO-6.7C	985	969	0.384	0.367

Table S2. The acidic properties of H-RHO-8.7, H-RHO-7.9C, H-RHO-7.3 and H-RHO-6.7C

Sample	Center of Acid Sites (°C)			Amount of Acid Sites (%) ^a		
	Weak	Medium	Strong	Weak	Medium and Strong	Total
H-RHO-8.7	169	217	506	9.3	64.8	74.1
H-RHO-7.9C	173	217	497	11.8	64.2	76.0
H-RHO-7.3	163	219	515	14.9	70.5	85.4
H-RHO-6.7C	174	229	542	18.6	81.4	100

^a The value was calculated by comparing the area of each acid sites with the total area of H-RHO-6.7C.

References:

1. T. Chatelain, J. Patarin, E. Fousson, M. Soulard, J. L. Guth and P. Schulz, Synthesis and characterization of high-silica zeolite **RHO** prepared in the presence of 18-crown-6 ether as organic template, *Microporous Mater.*, 1995, **4**, 231-238.
2. Q. Ke, T. Sun, H. Cheng, H. Chen, X. Liu, X. Wei and S. Wang, Targeted synthesis of ultrastable high-silica **RHO** zeolite through alkali metal-crown ether interaction, *Chem. - Asian J.*, 2017, **12**, 1043-1047.
3. Q. Ke, T. Sun, X. Wei, Y. Guo, S. Xu and S. Wang, Economical synthesis strategy of **RHO** zeolites with fine-tuned composition and porosity for enhanced trace CO₂ capture, *Chem. Eng. J.*, 2019, **359**, 344-353.
4. X. Bai, J. Zhang, C. Liu, S. Xu, Y. Wei and Z. Liu, Solid-state NMR study on dealumination mechanism of H-**MOR** zeolite by high-temperature hydrothermal treatment, *Microporous Mesoporous Mater.*, 2023, **354**, 112555.
5. I. Mochida, A. Yasutake, H. Fujitsu and K. Takeshita, Selective synthesis of dimethylamine (DMA) from methanol and ammonia over zeolites, *J. Catal.*, 1983, **82**, 313-321.
6. J. Han, J. Li, W. Zhao, L. Li, M. Chen, X. Ge, S. Wang, Q. Liu, D. Mei and J. Yu, Cu-**OFF/ERI** zeolite: Intergrowth structure synergistically boosting selective catalytic reduction of NO_x with NH₃, *J. Am. Chem. Soc.*, 2024, **146**, 7605-7615.
7. M. Moliner, C. Franch, E. Palomares, M. Grill and A. Corma, Cu-SSZ-39, an active and hydrothermally stable catalyst for the selective catalytic reduction of NO_x, *Chem. Commun.*, 2012, **48**, 8264-8266.
8. N. Kosinov, C. Auffret, G. J. Borghuis, V. G. P. Sripathi and E. J. M. Hensen, Influence of the Si/Al ratio on the separation properties of SSZ-13 zeolite membranes, *J. Membr. Sci.*, 2015, **484**, 140-145.